IOP PUBLISHING JOURNAL OF OPTICS
J. Opt. **15** (2013) 075101 (5pp) doi:10.1088/2040-8978/15/7/075101

Thermally tunable magnetic metamaterials at THz frequencies

Son Tung Bui[1], Van Dung Nguyen[1], Xuan Khuyen Bui[1], Thanh Tung Nguyen[2], Peter Lievens[2], YoungPak Lee[3] and Dinh Lam Vu[1]

[1] Institute of Materials Science, Vietnam Academy of Science and Technology, 18 Hoang Quoc Viet Road, Cau Giay District, Hanoi, Vietnam
[2] Department of Physics and Astronomy, KU Leuven, B-3001 Leuven, Belgium
[3] Quantum Photonic Science Research Center and Department of Physics, Hanyang University, Seoul 133-791, Korea

E-mail: thanhtung.nguyen@fys.kuleuven.be and lamvd@ims.vast.ac.vn

Received 25 February 2013, accepted for publication 24 May 2013
Published 20 June 2013
Online at stacks.iop.org/JOpt/15/075101

Abstract
We investigate theoretically and numerically the tunability of the magnetic property of metamaterial in the THz region via thermal control. One component of the meta-atom is InSb, playing an important role as an alterable metal. When the temperature of the InSb stack increases from 300 to 350 K, the resonance peak of the transmission spectra shows a shift from 0.6 to 0.85 THz accompanied by a stronger magnetic behavior. The *S*-parameter retrieval method realizes the tunability of the negative permeability achieved in the above heating range.

Keywords: tunable metamaterials, negative permeability, InSb

(Some figures may appear in colour only in the online journal)

1. Introduction

The study of artificially engineered materials, the so-called metamaterials (MMs), has grown rapidly and extensively since the first theoretical proposal by Veselago [1] and the first experimental demonstration by Smith [2]. The exotic abnormal properties of MMs have been employed in various applications, such as perfect absorbers [3–5], subwavelength imaging [6, 7], invisibility cloaking [8, 9] and slow light [10–13]. The operation regime has also been extended, from microwaves [4, 8] to the infrared [5, 9] and to the visible [6, 14]. Recently, researchers have been interested in how MMs can be dynamically and real-time controlled. The conventional metamaterial (MM) structure with determined geometrical parameters can operate only at a fixed frequency, which limits its actual applicability. In order to achieve tunable MMs, reconfigurable materials must be incorporated such that the electromagnetic responses can be controllable by various external means. So far, there have been several approaches proposed. One of the early manipulation techniques was realized by Chen *et al* [15]. The authors presented an active MM switch/modulator through external voltage control. Subsequently, another approach of tunability was confirmed using the electrical reorientation phenomenon in liquid crystals [16, 17]. In addition, semiconductor-integrated MMs were also proposed as a promising candidate. The intrinsic properties of natural semiconductors are flexibly and easily manipulated using various means, including temperature, electricity and optics. For instance, thermally or electrically tunable MMs were demonstrated based on the control of the carrier density in indium antimonide (InSb) [18, 19]. In addition, a thermally induced insulator–metal phase transition in vanadium dioxide (VO_2) was also employed to develop active MMs [20, 21]. Some different approaches are also of great promise, such as using the inter-subband transitions of semiconductors in semiconductor quantum wells [22] or ferrite dielectric materials [23].

The nature of negative permeability MMs can be described by the equivalent circuit model. The coupling

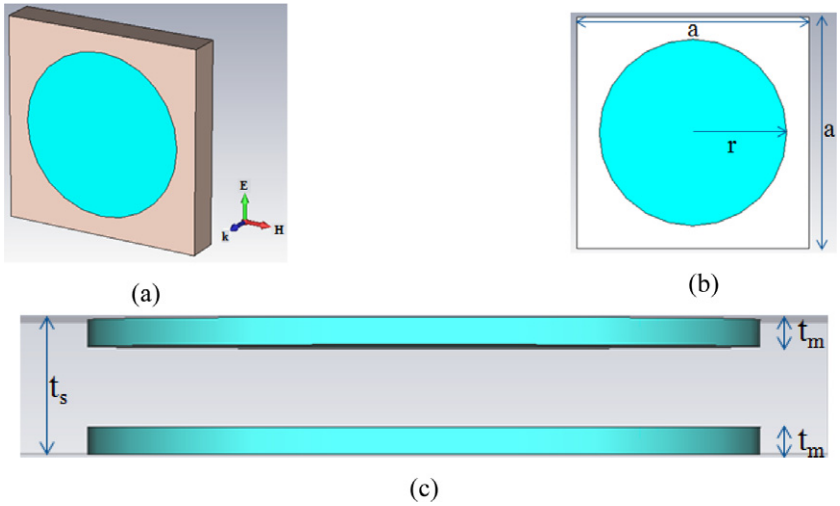

Figure 1. A unit cell of the dish structure, (a) perspective view with the electromagnetic polarization, (b) (**E**, **H**) plane and (c) (**k**, **E**) plane. Geometrical parameters are $a = 62\ \mu$m, $r = 25\ \mu$m, $t_s = 10\ \mu$m, $t_m = 2\ \mu$m.

between a LC resonator and an applied field produces a magnetic resonance. An enhancement of the diamagnetic phenomenon, appearing on the right side of the resonance frequency, yields a narrow negative permeability band. The magnetic resonance frequency is calculated by $\omega = \frac{1}{\sqrt{LC}}$, where L is the effective inductance and C is the effective capacitance. Hence, if one can control the value of either L or C, the resonance is actively shifted. One idea is the integration of a semiconductor into conventional MMs. According to the Drude model, the carrier density in a semiconductor depends solely on temperature. Consequently, the value of either the effective inductance or capacitance can be thermally manipulated. Based on the aforementioned argument, we propose a thermally tunable magnetic MM, using InSb as a mutable metal, in the THz region. Our design is a symmetric and simple structure that makes the MM insensitive to polarization, flexible and capable of scaling down.

2. Design and simulation

In the development of MMs, there have been two well-known magnetic metamaterial elements, the split-ring resonator (SRR) and the cut-wire pair (CWP) structure. However, the CWP structure has advantages over the SRR structure. Besides the simplicity of its geometry, planar CWP structures for a normal incident wave allow us to provide a negative permeability using only one layer. Therefore, based on the CWP structure, with a slight modification, the dish-pair (DP) structure was designed, as shown in figure 1. The improvement of the proposed structure is a highly symmetric geometry that makes the MM polarization-insensitive. The arrangement of dish layers and the dielectric layer is consistent with lithography fabrication techniques in the THz region, including evaporation and patterning processes. The DP MM consists of a periodic array of unit cells in the x and y directions with a periodicity of $a = 62\ \mu$m. Figure 1 shows an illustration of a unit cell of the DP structure. Each unit cell contains two identical dishes, symmetrically arranged in a dielectric spacer. The thicknesses of the dielectric and the metal are $t_s = 10\ \mu$m and $t_m = 2\ \mu$m, respectively. The radius of the dish is $r = 25\ \mu$m. The whole MM is placed in a reference medium, chosen as vacuum. The numerical simulations are performed using the commercial CST Microwave Studio. The propagation direction of incident electromagnetic wave is parallel to the axis of the dish while the (**E**, **H**) plane is normal, as shown in figure 1(a). The dielectric spacer is Pyrex glass with a dielectric constant of 4.82 and a loss tangent of 0.0054. Pyrex glass is a useful material in high-temperature applications. The dishes are made of InSb semiconductor. In the far infrared region, the permittivity of InSb can be determined according to the Drude model [18, 24].

$$\varepsilon = \varepsilon_\infty - \frac{\omega_p^2}{\omega^2 + i\gamma\omega}$$

where ε_∞ is the high-frequency dielectric constant, ω is the angular frequency, γ is the damping constant and ω_p is the plasma frequency. The plasma frequency is defined as $\omega_p = (\frac{Ne^2}{\varepsilon_0 m^*})^{\frac{1}{2}}$, in which N is the carrier density, e is the electronic charge, ε_0 is the vacuum permittivity and m^* is the effective mass of free carriers. In fact, the damping constant γ of InSb depends on the electron mobility μ as $\gamma = \frac{em^*}{\mu}$. Therefore, one might expect an influence of temperature on the damping constant that can affect the absorption of InSb. However, in the temperature range of interest between 300 and 350 K, within a frequency region from 0.1 to 1.5 THz, the electron mobility depends barely on temperature [25, 26]. For this reason, the influence of temperature on the damping constant can be neglected. The values of the parameters of InSb are $\varepsilon_\infty = 15.68$, $\gamma = 5 \times 10^{10}$ Hz, and $m^* = 1.37 \times 10^{-32}$ kg [18, 24].

3. Results and discussion

For InSb, the carrier density is determined by the formula $N = 5.76 \times 10^{14} T^{\frac{3}{2}} \exp(\frac{-0.13}{k_B T})$, where T is the absolute

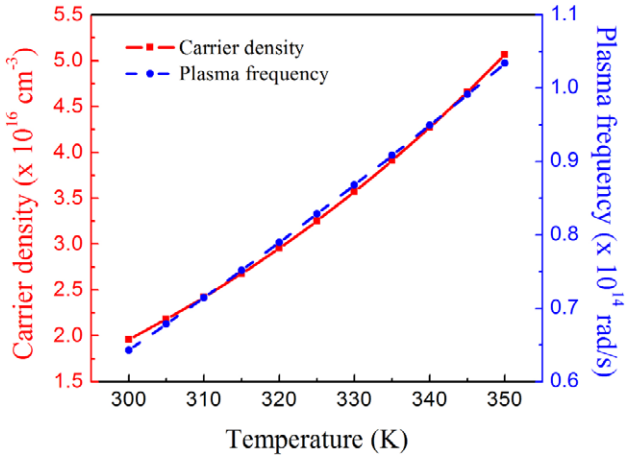

Figure 2. Calculated carrier density (red solid line) and plasma frequency (blue dashed line) of InSb according to temperature.

temperature and k_B is the Boltzmann constant [18, 24]. Hence, we can calculate the dependence of the plasma frequency on temperature. Figure 2 shows the calculated carrier density and plasma frequency of InSb according to temperature. An increase of temperature gives rise to an increased carrier density and plasma frequency. Consequently, InSb shows a more metallic feature, which plays an important role in constructing our thermally tunable MM.

Substituting these calculated results into the Drude model, we carried out the simulation at different temperatures. The simulated transmissions are shown in figure 3(a). The DP structure exhibits transmission dips in the spectra when an external field is applied. The phenomenon is well known, since the DP MM is a type of magnetic resonator. The coupling of the meta-atom to the **H** field produces a magnetic resonance leading to the narrow stop band. However, the attractive result is the shift of the transmission from 0.6 to 0.85 THz when InSb is heated from 300 to 350 K. Obviously, the magnetic behavior is tuned by controlling the temperature of InSb. The blue shift of the magnetic resonance can be explained using the equivalent *LC* model. The resonance frequency can be approximately described as $\omega = \frac{1}{\sqrt{LC}}$. Besides the usual inductance, the kinetic inductance also contributes to the total inductance of a conductor [27]. As mentioned above, the carrier density increases on raising the temperature. An enhancement of the carrier density reduces the value of the kinetic inductance, as in the formula $L_K = \alpha \frac{m}{Ne^2}$, where m is the electron mass and α is a factor depending on the geometry of the conductor. (In the case of our DP conductor, the formula for α is $\alpha = \frac{\pi}{2t_m}$. The formula is calculated based on the method in [27].) Therefore, the magnetic resonance should shift to higher frequencies, as shown in the transmission spectra. The losses as a function of the frequency at 300, 325 and 350 K are presented in figure 3(b). The absorbance peak at these temperatures is in the range from 0.4 to 0.5. The loss properties of the DP structure are consistent with previous research on the CWP structure [28]. Since the DP structure design originates from the CWP structure, the magnitude of absorbance must be similar in both structures.

In order to verify the existence of a negative permeability, the standard retrieval method is performed [29]. Figure 4 shows the retrieved permeability according to temperature. It is clearly seen that negative permeability is achieved in a temperature range from 300 to 350 K. In addition, the magnitude of the permeability is strengthened at the resonance position when the temperature is raised. Owing to the stronger magnetic behavior, the negative permeability band becomes gradually wider.

The stronger magnetic behavior can be explained by the enhancement of the carrier density. While the unit structure is constant, the increase of the carrier density leads to a stronger anti-parallel current. Consequently, the magnetic resonance strength and the permeability are enhanced. In order to verify this phenomenon, figure 5 presents the distribution of the induced magnetic energy at the resonance frequency for different temperatures: 300, 325 and 350 K. Obviously, the induced magnetic energy increases when InSb is heated, which confirms the strengthening of the magnetic behavior.

Figure 6 is the electric energy distribution at the resonance frequency according to different temperatures. The

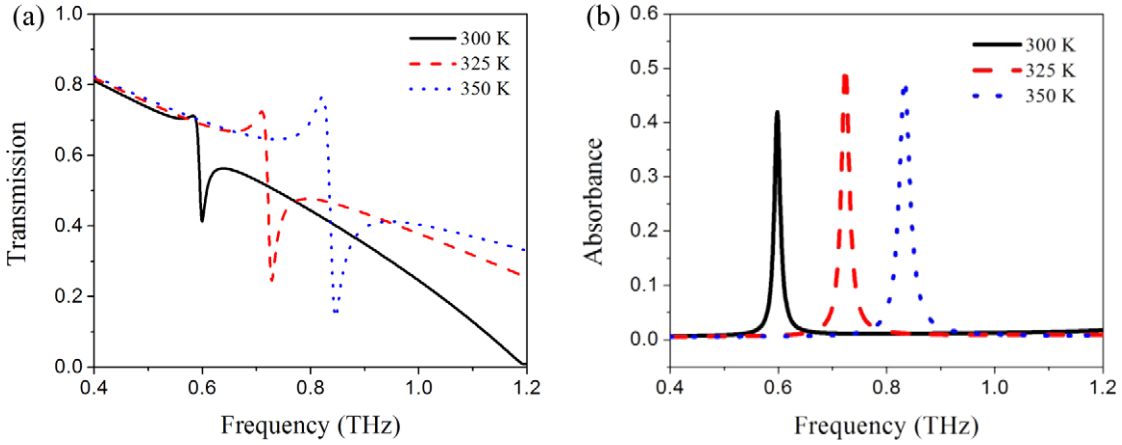

Figure 3. Dependence of the simulated (a) transmission and (b) absorbance on temperature.

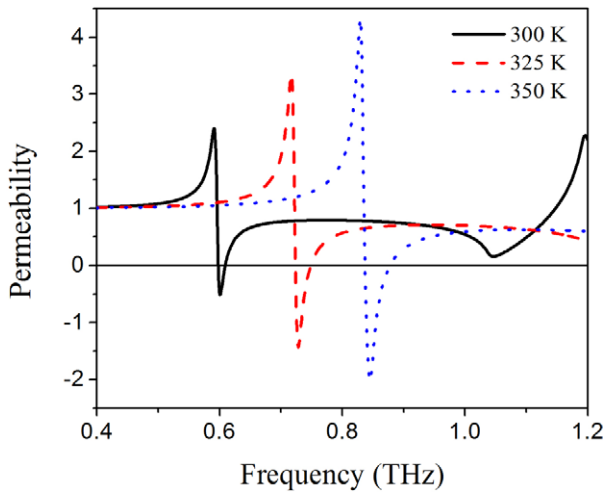

Figure 4. Real part of the effective permeability according to temperature.

electric energy mainly locates at the ends of the disk along the **E** direction. The phenomenon is consistent with the magnetic nature of the resonance. Owing to the strong coupling between the MM and the magnetic component of the electromagnetic field, anti-parallel currents are generated on paired disks along the **E** direction. Therefore, charges are accumulated at the ends of the disk that lead to strong electric energy there. The dependence of electric energy on temperature is also presented in figure 6. The magnitude of electric energy decreases when the temperature increases from 300 to 350 K.

4. Conclusions

We proposed a simple, thermally tunable magnetic metamaterial using semiconducting InSb. The tunability in the far infrared region of the negative permeability and the stronger magnetic behavior were explained clearly by the enhancement of the carrier density when InSb is heated from 300 to 350 K. The design of the structure and the manipulation mechanism are very simple, giving it the potential for applications. Furthermore, with a diversified choice of semiconductors, our approach might be useful not only in the far infrared but also in the visible region.

Acknowledgments

This work was supported by the joint research project between the Vietnam National Foundation for Science and Technology

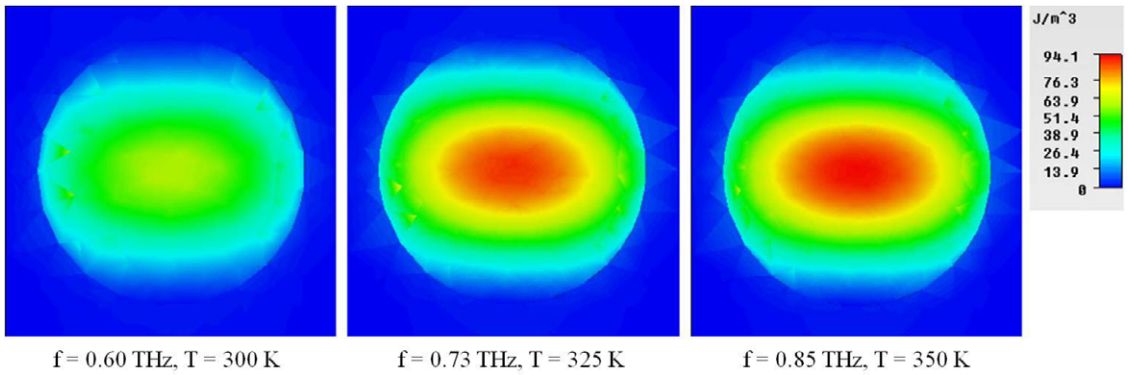

Figure 5. Magnetic energy distribution at the resonance frequency according to temperature 300 K (at $f = 0.60$ THz), 325 K (at $f = 0.73$ THz) and 350 K (at $f = 0.85$ THz).

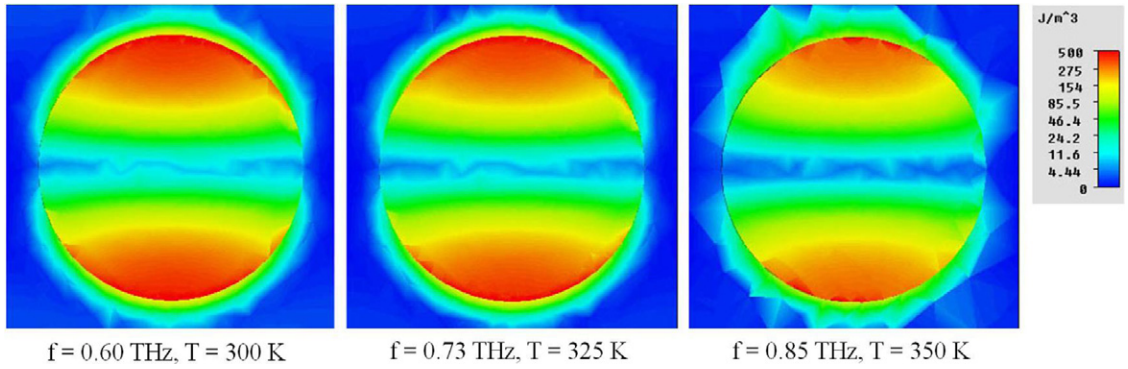

Figure 6. Electric energy distribution at the resonance frequency according to temperature 300 K (at $f = 0.60$ THz), 325 K (at $f = 0.73$ THz) and 350 K (at $f = 0.85$ THz).

Development (NAFOSTED) and the Research Foundation Flanders (FWO) FWO.2011.35.

References

[1] Veselago V G 1968 The electrodynamics of substances with simultaneously negative values of ε and μ *Sov. Phys.—Usp.* **10** 509

[2] Smith D R, Padilla W J, Vier D C, Nemat-Nasser S C and Schultz S 2000 Composite medium with simultaneously negative permeability and permittivity *Phys. Rev. Lett.* **84** 4184

[3] Landy N I, Sajuyigbe S, Mock J J, Smith D R and Padilla W J 2008 Perfect metamaterial absorber *Phys. Rev. Lett.* **100** 207402

[4] Ding F, Cui Y, Ge X, Jin Y and He S 2012 Ultra-broadband microwave metamaterial absorber *Appl. Phys. Lett.* **100** 103506

[5] Dayal G and Ramakrishna S A 2012 Design of highly absorbing metamaterials for infrared frequencies *Opt. Express* **20** 17503

[6] Fang N, Lee H, Sun C and Zhang X 2005 Sub-diffraction-limited optical imaging with a silver superlens *Science* **308** 534

[7] Scarborough C P, Jiang Z H, Werner D H, Rivero-Baleine C and Drake C 2012 Experimental demonstration of an isotropic metamaterial superlens with negative unity permeability at 8.5 MHz *Appl. Phys. Lett.* **101** 014101

[8] Schurig D, Mock J J, Justice B J, Cummer S A, Pendry J B, Starr A F and Smith D R 2006 Metamaterial electromagnetic cloak at microwave frequencies *Science* **314** 977

[9] Pawlik G, Tarnowski K, Walasik W, Mitus A C and Khoo I C 2012 Infrared cylindrical cloak in nanosphere dispersed liquid crystal metamaterial *Opt. Lett.* **37** 1847

[10] Liu N, Liu H and Giessen H 2009 Stereometamaterials *Nature Photon.* **3** 157

[11] Jang M S and Atwater H 2011 Plasmonic rainbow trapping structures for light localization and spectrum splitting *Phys. Rev. Lett.* **107** 207401

[12] Zhu L, Meng F Y, Fu J H, Wu Q and Hua J 2012 Multi-band slow light metamaterial *Opt. Express* **20** 4494

[13] Chen C K, Lai Y C, Yang Y H, Chen C Y and Yen T J 2012 Inducing transparency with large magnetic response and group indices by hybrid dielectric metamaterials *Opt. Express* **20** 6952

[14] Nehmetallah G, Aylo R, Powers P, Sarangan A, Gao J, Li H, Achari A and Banerjee P P 2012 Co-sputtered SiC + Ag nanomixtures as visible wavelength negative index metamaterials *Opt. Express* **20** 7095

[15] Chen H T, Padilla W J, Zide J M O, Gossard A C, Taylor A J and Averitt R D 2006 Active terahertz metamaterial devices *Nature* **444** 597

[16] Minovich A, Neshev D N, Powell D A, Shadrivov I V and Kivshar Y S 2010 Tunable fishnet metamaterials infiltrated by liquid crystals *Appl. Phys. Lett.* **96** 193103

[17] Zhang F, Zhao Q, Zhang W, Sun J, Zhou J and Lippens D 2010 Voltage tunable short wire-pair type of metamaterial infiltrated by nematic liquid crystal *Appl. Phys. Lett.* **97** 134103

[18] Bai Q, Liu C, Chen J, Cheng C, Kang M and Wang H T 2010 Tunable slow light in semiconductor metamaterial in a broad terahertz regime *J. Appl. Phys.* **107** 093104

[19] Miao X, Passmore B, Gin A, Langston W, Vangala S, Goodhue W, Shaner E and Brener I 2010 Doping tunable resonance: toward electrically tunable mid-infrared metamaterials *Appl. Phys. Lett.* **96** 101111

[20] Wen Q Y, Zhang H W, Yang Q H, Xie Y S, Chen K and Liu Y L 2010 Terahertz metamaterials with VO_2 cut-wires for thermal tunability *Appl. Phys. Lett.* **97** 021111

[21] Wen Q Y, Zhang H W, Yang Q H, Chen Z, Long Y, Jing Y L, Lin Y and Zhang P X 2012 A tunable hybrid metamaterial absorber based on vanadium oxide films *J. Phys. D: Appl. Phys.* **45** 235106

[22] Gabbay A and Brener I 2012 Theory and modeling of electrically tunable metamaterial devices using inter-subband transitions in semiconductor quantum wells *Opt. Express* **20** 6584

[23] He G, Wu R X, Poo Y and Chen P 2010 Magnetically tunable double-negative material composed of ferrite-dielectric and metallic mesh *J. Appl. Phys.* **107** 093522

[24] Han J and Lakhtakia A 2009 Semiconductor split-ring resonators for thermally tunable terahertz metamaterials *J. Mod. Opt.* **56** 554

[25] Rode D L 1971 Electron transport in InSb, InAs, and InP *Phys. Rev.* B **3** 3287

[26] Zhu J, Han J, Tian Z, Gu J, Chen Z and Zhang W 2011 Thermal broadband tunable terahertz metamaterials *Opt. Commun.* **284** 3129

[27] Linden S, Enkrich C, Dolling G, Klein M W, Zhou J, Koschny T, Soukoulis C M, Burger S, Schmidt F and Wegener M 2006 Photonic metamaterials: magnetism at optical frequencies *IEEE J. Sel. Top. Quantum Electron.* **12** 1097

[28] Wakatsuchi H, Greedy S, Christopoulos C and Paul J 2010 Customised broadband metamaterial absorbers for arbitrary polarization *Opt. Express* **18** 22187

[29] Chen X, Grzegorczyk T M, Wu B I, Pacheco J and Kong J A 2004 Robust method to retrieve the constitutive effective parameters of metamaterials *Phys. Rev.* E **70** 016608